ELSEVIER

International Journal of Mass Spectrometry 190/191 (1999) 69–80

International Journal of Mass Spectrometry

Optimum phase angle for laser desorption ion trap mass spectrometry is dependent on the number of ions produced

Damon B. Robb[1], Michael W. Blades*

Department of Chemistry, University of British Columbia, Vancouver, British Columbia V6T 1Z1, Canada

Received 5 October 1998; accepted 12 April 1999

Abstract

For laser desorption sampling within a quadrupole ion trap, the phase and amplitude of the rf potential used to trap the ions, as well as the helium bath gas pressure, are important factors governing sensitivity. This article is concerned with investigating the dependence of trapping efficiency on the phase angle at the time that the laser fires. New data have been acquired demonstrating how the distribution of phase values that yield successful trapping, as well as the optimum phase for trapping, vary with the number of ions produced during the laser desorption event. It will also be shown that the position on the probe where the ions are created is a further factor in determining the optimum phase for trapping. Additional evidence taken from the laser desorption mass spectrometry literature will be used to propose a model for the dependence of the signal intensity versus phase relationship on the number of ions produced. It will be argued that trends in the data observed here are due to the effects of Debye shielding that accompany the desorption of substantial quantities of positive and negative ions. The dependency of the optimum phase angle on the position on the probe where the ions originate is not well understood at this time. Last, it will be shown how the pressure of helium within the trap does not influence the optimum phase value for trapping, but the effects of the bath gas pressure on trapping efficiency and fragmentation are interesting and will be discussed briefly. (Int J Mass Spectrom 190/191 (1999) 69–80) © 1999 Elsevier Science B.V.

Keywords: Ion trap; Laser desorption; Trapping efficiency

1. Introduction

In order to optimize the sensitivity for quadrupole ion trap mass spectrometers utilizing ion sources located external to the central trapping volume, it is essential that the factors governing trapping efficiency be well understood. Key experimental parameters that may be varied to control trapping efficiency include the amplitude (q_z) and phase of the rf potential used to trap the ions, as well as the pressure of helium bath gas within the trap. There is some confusion in the literature, however, regarding the mechanisms by which the first two parameters affect trapping efficiency. In this laboratory, with the advent of polythiophene films for laser desorption samples [1], many experiments were undertaken seeking to better understand the trapping process and to clarify these inconsistencies. Some of our findings regarding the dependence of laser desorption ion trap mass spectrometry (LD-ITMS) signal intensities on q_z have recently been

* Corresponding author.

[1]Present address: University Center for Pharmacy, A. Deusinglaan 1, 9713 AV Groningen, The Netherlands.

Dedicated to J.F.J. Todd and R.E. March in recognition of their original contributions to quadrupole ion trap mass spectrometry.

PII S1387-3806(99)00061-5

reported [2]. In this article, we will present and discuss the results of a study examining the relationship between trapping efficiency and the phase angle of the rf potential at which ions are desorbed by the laser.

Several prior laser desorption studies report measurements of sensitivity for ions injected into an ion trap as a function of phase angle, but there is no consensus regarding what the value is for optimum trapping [2–7]. The results of simulations performed in our laboratory [8], as well as those reported in the literature [9,10], indicate that the optimum phase angle for trapping ions is a function of the rf amplitude (q_z), and the kinetic energy of each injected ion. Kinetic energy of injected ions is a variable that is not readily controlled in LD-ITMS experiments, so it comes as no surprise that researchers employing unique experimental arrangements have reported different results. Significantly, to the best of our knowledge, there have been no published attempts to correlate the real LD-ITMS experimental data with the results of the ion injection simulations. Hence, it has not been shown that the variation between experimental results is due solely to differences in q_z, or the kinetic energies of the ions, as could be surmised from the simulations. It may then be that any number of previously unconsidered factors contribute to the trapping process, and thus influence the value of the optimum phase angle for confining injected or desorbed ions.

Early results from this laboratory confirmed the dependence of the LD-ITMS signal intensity on the phase of the rf potential and q_z; however, there were some troubling inconsistencies in the data. Specifically, it was found that for seemingly identical experimental conditions (same sample type, q_z, buffer gas pressure, and laser irradiance) the optimum phase angle varied widely between repeats of the same experiment, often by 90° or more. These inconsistencies were at first believed to be the result of imperfect calibration of the electronics governing the timing of the experiments, but repeated measurements always confirmed that this was not the case. The only significant source of uncertainty in the calibration scheme is the jitter in the laser firing time, which, at no more than ± 30 ns, corresponds to a maximum uncertainty in the phase calibration of $\pm 10°$. The idea that the variation could be due to a real ion trapping effect was originally dismissed with little thought. In retrospect, though, it is clear that because the experimental apparatus was sound, the discrepancies between the results of repeats of the same experiments must have been due to real variables that were left unaccounted.

After several months of futilely attempting to resolve this problem, two previously overlooked experimental variables were empirically determined to be responsible, at least in part, for the observed inconsistencies. First, the optimum phase angle for a given value of q_z was found to depend on the quantity of ions desorbed during the laser pulse. Based upon new data presented in this article, and related evidence in the laser desorption mass spectrometry literature, a plausible mechanism for this dependence may be inferred. In the following discussion, it will be argued that trends observed in the present investigation are due to the collective ability of the desorbed ion plume to provide shielding of the ions within the plume from the applied electric field used to confine the ions. This phenomenon, known as Debye shielding, is typically associated with plasmas consisting of positive ions, electrons, and neutral species [11]. In the past, Debye shielding has been demonstrated to allow laser desorbed atomic ions generated from metal surfaces to penetrate retarding potential barriers greatly exceeding the initial kinetic energy of the ions [12]. For instance, it was found that Debye shielding exhibited by quasineutral populations was sufficient in some cases to allow ions on the order of 1 eV to penetrate retarding potentials as high as 500 V. Evidence from another early study suggests that the effects of Debye shielding in laser desorption are not limited to plasmas generated from metal targets, but may also be observed for ion plumes generated from ionic substances by thermal processes [13], such as those resulting from the low irradiance laser desorption technique used here.

Quite unexpectedly, the optimum phase angle for trapping was also found to vary with the lateral position of the lens used to focus the laser energy onto

the sample surface. The origins of this dependency are not well understood, though a tentative explanation is offered in the discussion. An additional experiment demonstrated that the phase relationship does not depend on the pressure of the helium buffer gas; however, the effects of buffer gas pressure on fragmentation and sensitivity in LD-ITMS are noteworthy and will be discussed briefly.

2. Experimental

The home-built instrument used for the experiments presented in this section has been described in detail elsewhere [1,2]. The apparatus consists of a set of stainless-steel ion trap electrodes with ideal quadrupole geometry (i.e. the endcaps are not "stretched"), encased within a vacuum manifold into which helium bath gas was introduced at variable pressures. The pressure within the manifold and the ion trap was the same, as the trap was not sealed. Oppositely aligned 2.5 mm holes were drilled into the ring electrode, allowing for direct sampling by a PRA Laser Inc. (London, Ont.) UV-12 nitrogen laser from the sample probe. The probe was inserted through a vacuum interlock and aligned such that the surface of the sample was flush with the inner surface of the ring. The output from a laser was focused by a 30.00 cm focal length silica planoconvex lens through a quartz window in the manifold.

User-written programs running on a 133 MHz Pentium computer controlled the experiments. Instrument control and data processing software was written in Microsoft QUICKBASIC, version 4.5. The computer was equipped with an RC Electronics (Santa Barbara, CA) model ISC-16 analog-to-digital converter (ADC), a QuaTech (Akron, OH) PBX-721 data acquisition parallel expansion board, and a QuaTech DM12-10 digital-to-analog converter (DAC). The rf quadrupole supply used was an Extranuclear Laboratories Inc. (Pittsburgh, PA) model number 011-1, modified for operation from 0.6 to 3.0 MHz. Capacitance matching was achieved using a High-Q Head model number 012-16, also from Extranuclear Laboratories. The maximum output of the rf supply was $\sim$3000 V (zero-to-peak), and the frequency was tuned to 0.967 MHz. The amplitude of the rf potential was governed by the output of the DAC, which was sent to the "external command" connection of the quadrupole controller. A Stanford Research Systems (Palo Alto, CA) model SRS DG535 digital delay generator was used to control the bulk delay between when the initial DAC command set the rf amplitude and when the laser fired. A delay of 5 ms ensured that the amplitude of the rf potential had stabilized before the ions were desorbed.

The trigger from the digital delay generator was sent to a zero-crossing detector built by the Electrical Services Shop (Chemistry Dept., U.B.C.). This device monitored the rf via an antenna, and, once enabled, detected the next positive going zero crossing of the rf voltage. A trigger was sent to the laser after the zero crossing was detected at a small adjustable delay relative to the period of the rf. This allowed for the laser firing time to be synchronized with the phase angle of the rf potential. A 400 MHz Tektronix (Wilsonville, OR) model TDS 380 digital oscilloscope was employed to correlate the delay setting of the zero-crossing detector with the phase angle at which the laser fired. This was accomplished by comparing the signal from the antenna placed near the ring electrode to the signal from a fast photodiode sampling a portion of the laser pulse. All connections were terminated into 50 Ω to ensure fast risetimes. The antenna signal was also corrected for the $+90°$ phase shift resulting from the capacitive pickup. Uncertainty in the phase measurements is due primarily to jitter in the laser firing time, which was measured to be no more than $\pm$30 ns, corresponding to a maximum phase uncertainty of $\pm 10°$.

After the laser fired and the desorbed ions were initially trapped, the rf potential amplitude was held constant for a period of 10 ms to allow for the ions to be cooled by collisions with the helium buffer gas. Subsequent to the cooling period, the rf potential was ramped to generate a mass spectrum of the trapped ions by the mass-selective instability operating mode [14]. The ejected ions were detected using an ETP (Sydney, Australia) model AF138 electron multiplier held at -1.7 kV. The signal from the detector was

then amplified with a gain of 10^7 V/A by a Kiethley (Cleveland, OH) model 428 current amplifier, and the amplified signal was sampled by the ADC with a period of 4 μs over the duration of the rf ramp.

For these experiments, series of laser desorption mass spectra were collected under various conditions as a function of the phase angle of the rf potential used to trap the ions. Note that zero degrees has been defined here to be the phase angle at the positive going zero crossing of the rf potential. The amplitude of the trapping potential was constant for all the trials, and was calculated from $q_z = 0.1$ for the tetrabutylammonium (TBA) molecular ion (*m/z* 242). For each series of data collected, spectra were acquired for 25 phase angles spanning one rf cycle. To compensate for random fluctuations in ion production between laser shots, 30 spectra were acquired and averaged for each phase angle at a rate of 5 spectra per second.

All the data presented in this section came from a polythiophene film [15] prepared as described previously [1,8]. TBA perchlorate was the supporting electrolyte used for the preparation for the film that provided the ions to be analyzed in these studies. Upon drying, a residue of the electrolyte ions remains intermixed with the polythiophene; hence, the sample films are impregnated with both TBA and perchlorate ions from the electrolyte solution.

A series of neutral density filters were used to attenuate the nitrogen laser energy output at 337 nm to $\sim$30 μJ. The lens focused the laser pulse to an ellipse of approximately 400 μm $\times$ 200 μm, leading to a calculated irradiance of $\sim 5 \times 10^6$ W/cm^2 at the surface of the sample. The lens was mounted on an *x–y–z* translation stage, and one experiment involved collecting data with the lens position set to different lateral positions. By translating the lens from side to side, the focal spot of the laser beam could be positioned at varying locations on the probe tip surface. The spatial arrangement of the ion trap relative to the laser is such that lateral translation of the lens causes the focal spot of the laser to move along the axial direction of the trap, with the radial position remaining constant. Initially, the lens position was adjusted such that the laser impinged on the outermost region of the probe tip (1.8 mm diameter). Ion production thus was achieved from a position on the probe that was displaced slightly toward one of the endcaps from the axial origin of the trap. Several sets of spectra were collected with the lens set to this position, then the lens was shifted 0.5 mm back toward the laser beam axis and additional data were acquired with the laser focused to an area near the center of the probe. The distance from the lens to the sample along the laser beam axis was not varied, so the focal area and the laser irradiance were constant.

The pressure of helium in the manifold was held at 1 mTorr for all the experiments, except for the final study where it was varied over a range of 0.5 mTorr to approximately 8 mTorr. The pressure in the manifold was directly measured with a Balzers model PKG 020 pirani-cold cathode gauge meter, equipped with a model IKR 020 cold cathode gauge head; however, cold cathode gauges are sensitive to gas composition and do not provide absolute pressure measurements. Accordingly, a capacitive manometer (Type 120 MKS Baratron® Vacuum Gauge) which provides absolute pressure measurements was used to calibrate the cold cathode gauge meter.

3. Results and discussion

3.1. Dependence of the phase for optimum trapping efficiency on ion production

Fig. 1 displays a series of LD-ITMS spectra of TBA collected as a function of the phase angle at which the laser fired, with q_z held constant. The dependence of signal intensity on phase is clear from the data. The peaks at *m/z* 242 are due to the TBA molecular ion, and the other major peaks in the spectra are due to TBA fragments, for which structural assignments have been made elsewhere [16,17]. The spectra displayed in Fig. 1(a) were collected from 750 of the first laser shots on the sample surface, when the ion production per laser shot was relatively high. To evaluate the effect of the ion yield per laser shot on trapping behavior, the sample was subjected to thousands of laser shots so that ion production was

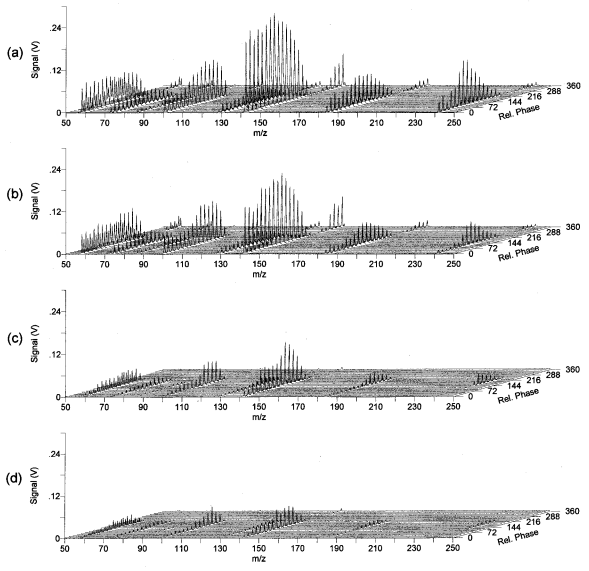

Fig. 1. Series of laser desorption mass spectra of tetrabutylammonium (TBA) acquired as a function of the phase angle at the time of the laser pulse. The data in plots (a)–(d) were collected at increasing stages of decay of the ion production per laser shot from the sample film. The calibration of the *z* axis is relative. Unless indicated otherwise, all other plots with a phase axis are calibrated absolutely.

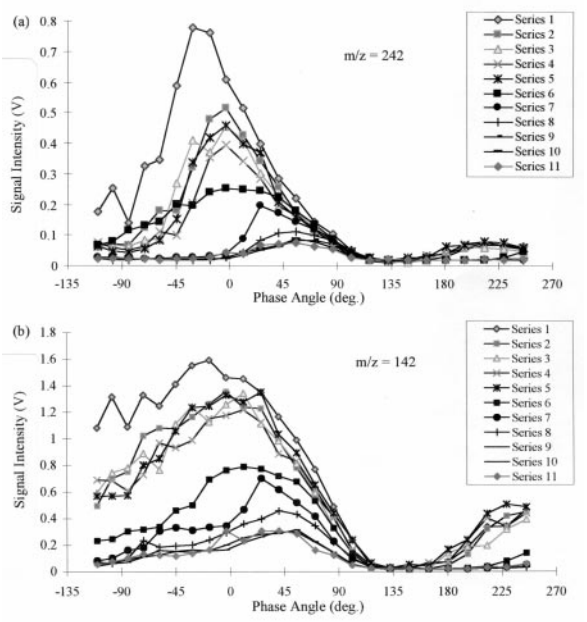

Fig. 2. Integrated signal for the (a) TBA molecular ion (*m/z* 242) and (b) one of the TBA fragment ions (*m/z* 142) collected as a function of phase angle and the total ion yield per laser pulse. Series 1 was acquired from 750 of the first laser shots on the film. The other series were acquired at increasing stages of decay of the ion production per laser shot from the film. The final data set, series 11, was collected after the film had previously been subjected to 28 000 shots on the same position.

gradually diminished and additional spectral series were acquired periodically. The series of spectra in Fig. 1(b)–(d) were collected at increasing stages of decay of the laser desorption ion yield, with the final series shown being acquired after more than 28000 shots on the same sample position. Eleven such series were acquired in all; the results of this study are summarized in Fig. 2(a) and (b).

There are two trends that are immediately conspicuous in Fig. 2: as the ion production from laser desorption diminishes (evidenced by a decrease in signal intensity over all phases), the peak phase angle for trapping becomes more positive, and the distribution of phases where ions are successfully trapped narrows. As well, for each series of spectra there is a cutoff phase where no more ions are trapped. The cutoff phase has a constant value of just greater than 90° for all the trials. A comparison between Fig. 2(a) and (b) shows that this behavior is followed by both the TBA molecular ion and its fragment at *m/z* 142. It is apparent that if the two trends were to continue, as fewer ions are produced, the distribution of acceptable phases would continue to narrow and the optimum phase for trapping would increase until it eventually equaled the unvarying cutoff phase. This is evident from Fig. 3, a summary plot of the peak integrated *m/z* 242 signal intensity for each series versus the phase angle at which the data was acquired. This plot plainly illustrates the positive shift that occurs in the optimum phase angle as the quantity of ions produced by each laser pulse decreases.

Before discussing the probable causes of the trends observed in the experimental data, it is first necessary to review a model of the trapping process which has developed from the simulations cited previously. The two simulation studies published recently considered the problem of trapping positive ions injected from an endcap electrode [9,10]. The mechanisms arising out of each investigation for the dependence of trapping

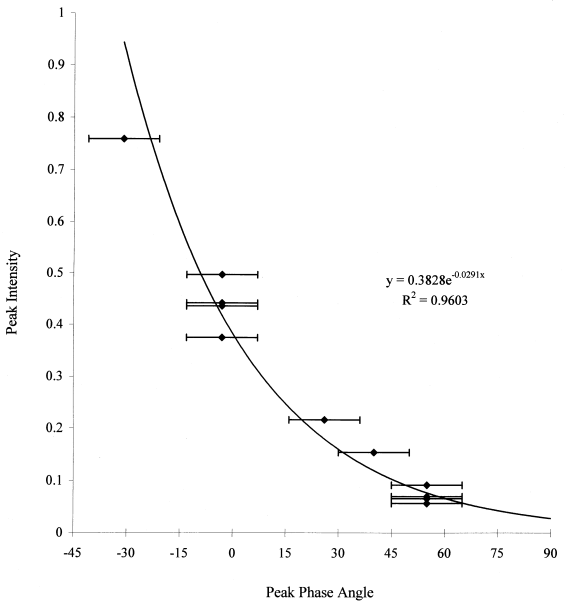

Fig. 3. Summary plot of the peak integrated *m/z* 242 signal intensity for each series vs. the phase angle at which the data was acquired. The optimum phase for trapping for series 1–11 depends on the mean number of ions produced from the sample by the laser. The error bars on the *x* axis correspond to the uncertainty in the phase angle calibration, ±10°.

efficiency on the initial phase of the rf potential are consistent with each other. The results of both studies indicate that, for ions with zero initial velocity, the ions may only penetrate the trapping volume if they are created when there is a negative potential on the ring electrode (phase angles from 180° to 360°). For all values of q_z, successful trapping may only occur when the phase upon injection is around 270°, at which the ions accumulate a minimum of kinetic energy upon reaching the trap center. The motion of the ions that are ultimately trapped is oscillatory, bounded in the axial dimension by the opposing endcaps, although the limits of displacement are much narrower in the radial dimension. Regarding the fate of ions created during the remainder of the rf cycle, positive ions introduced at phases when there is a positive potential on the ring (from 0° to 180°) are excluded entirely from the inner volume of the ion trap, because they initially face an uphill potential barrier. Ions introduced to the quadrupole field at phases less than 270°, but greater than 180°, experience excessive acceleration during the negative portion of the rf cycle, have too much energy upon crossing the trap center, and are lost at the opposite endcap. Ions created at phases greater than 270°, but less than 360°, are also initially accelerated towards the trap center, but are repelled back into the electrode that they originated from when the potential on the ring electrode becomes positive.

Another key finding of the simulations is that as the velocity initially possessed by the injected ions increases, the optimum phase angle for trapping increases from 270°, because less acceleration is required for the ions to penetrate sufficiently far into the trap so that they will not be pulled back into the endcap when the rf potential switches polarity. Ions created at 270° with nonzero initial kinetic energy are lost at the far side of the ion trap, because the combination of their initial energy and the velocity gained due to acceleration during the next quarter of the rf cycle is excessive.*

Results from the simulations performed in this laboratory are also consistent with those of the two described previously [8]. One key difference between the simulations is that, in this instance, the investigation considered ions injected from the ring electrode instead of an endcap. The results for the dependence of the trapping mechanism on the initial rf phase angle were shifted by 180° from those discussed above, because, relative to the potential at the trap center, the potentials on the ring and on the endcaps are out of phase by 180°. Hence, the optimum phase angle for trapping ions injected from the ring electrode was 90° for ions created with zero kinetic energy, or slightly greater for those with some small initial velocity.

Returning to the earlier analysis of the LD-ITMS experiments, it is now profitable to compare the results from these with those of the simulations.

* Note that none of the simulations considered thus far have been able to accurately account for the effects of ion–ion interactions, one of which may be Debye shielding. It is plain to see, then, that the results of the simulations are only meaningful for the ideal case of a single ion unaffected by other charged particles, acting under the exclusive influence of the electric fields generated by the potentials applied between the trap electrodes.

Reiterating, if the experimentally observed trends were to continue, then, in the limit of only one ion being produced, the data suggest that the ion may only be trapped when created at a phase slightly greater than 90°. This finding agrees exactly with the results predicted by the simulations for one ion injected with nominal initial kinetic energy, a starting condition that may reasonably be assumed to hold for an ion created by a thermal laser desorption process. For the problem of trapping ions created outside of the central volume of the quadrupole ion trap, this is the first reported instance of congruence between the results obtained from real experiments and those from simulation studies. The evidence thus suggests that the simulations accurately reflect ion trapping behavior, albeit only for the seemingly unrealistic situation where there are no significant effects resulting from ion–ion interactions. The problem remains to explain the effects that are experimentally observed to accompany the production of substantial quantities of both positive and negative ions.

The variance observed in Fig. 2 with the number of ions produced indicates that the ions themselves affect the trapping process. Other studies have shown that ions within quasineutral plumes resulting from laser desorption can be shielded from the influence of external electric fields [12,13]. If it is assumed that this phenomenon, Debye shielding, also contributes to the process governing the trapping of the TBA ions analyzed here, then it is possible to describe a mechanism that accounts for the discrepancies between the results of the experiments and the simulations. The principle effect that can be ascribed to Debye shielding is an added delay between the time that ions are formed and when they experience the full amplitude of the applied rf field. To understand how this may come about, one must consider the processes that accompany the arrival of the laser pulse. First, a plume consisting, at least in part, of TBA and perchlorate ions is desorbed as a result of rapid heating of the sample by the laser pulse. The immediate collective action of the particles within the quasineutral ensemble is to arrange themselves such that Coulombic repulsion is minimized. One of the ensuing effects is that ions within the plume are shielded from external electric fields; only the outer-shell of the plume is left unshielded. The thickness of this layer is specified by the Debye length, which depends upon the density of charged particles within the plume, among other factors [11]. Those ions within the plume that are shielded from the rf field will diffuse away from the probe tip, into the trapping volume, at the velocities imparted to them during the desorption event (typical reported velocity values range from 400 to 1000 m/s [18–20]). Ions that are affected by the external electric field will be accelerated away from the rest of the ions, at a rate dependent upon the instantaneous magnitude of the applied rf potential. We thus have a system characterized by an inner-core of shielded ions diffusing in a field-free manner, that will ultimately be dispersed due to the normal expansion of the plume and the invasive effects of the quadrupole field.

A predictable consequence of the processes described above is that there will be a distribution in time over which desorbed TBA ions first experience the full effects of the rf field. The shape of this distribution will depend upon the rate at which deshielding of ions within the plume occurs as it is dispersed. The rate of dispersal can be expected to be directly related to the instantaneous magnitude of the rf potential. As well, the dispersal rate must be inversely related to the density of the plume, because the Debye length specifying the depth of penetration of external electric fields into the plume is reduced for higher charged particle densities. Both the instantaneous magnitude of the applied potential and the density of the plume vary over time, so the dispersal rate of the plume cannot be easily predicted. In short, the factors governing the rate at which the ion plume is dispersed are complex, and it is currently not possible to predict the delay subsequent to the laser firing event at which the greatest number of ions will be deshielded.

The measured dependence of the TBA signal intensity on the phase at the time of the laser firing is a function of the distribution in time over which the desorbed ions first experience the rf field. If the presupposition is valid that unshielded ions at the ring electrode are only efficiently trapped when introduced

at a phase angle of around 90°, then, from the data displayed in Fig. 2, it is possible to infer what the distribution for each series was likely to have been. For example, the peak ion signal for series 1 was obtained when the laser fired at ~−30°, a negative shift of 120° (equivalent to roughly 350 ns) from the theoretical optimum phase for trapping unshielded ions. We can therefore infer that the greatest number of ions were deshielded at approximately 350 ns after the laser fired. Signals observed at phases less than the optimum (<−30°) came from ions that had been deshielded at delays greater than 350 ns. Conversely, those observed at phases greater than the optimum value came from ions deshielded at delays less than 350 ns. The cutoff phase can also be explained: when the laser fired at a time such that the rf phase was just greater than the cutoff value, for all the data series collected here, no ions were trapped because all the ions were deshielded and lost in a period less than the time it took for the rf phase to cycle through again to the optimum value of ~90°.

A key factor that must be considered in evaluating the accuracy of this model is the distance into the trap that the ions penetrate while they are shielded. This is because the assumption that ions are most efficiently trapped when deshielded at 90° may only hold if they start at the outer edge of the quadrupole field (i.e. at the ring electrode). Assuming an average velocity of 700 *m/s*, ions drifting for 350 ns before experiencing the quadrupole field will have traversed only 0.24 mm during the shielding period. This displacement is likely insignificant insofar as it affects the value of the phase angle for which ions are most likely to be trapped.

The delay between when the laser fires and when the peak number of ions are first influenced by the quadrupole field is a function of the quantity of ions produced during the laser shot. Shielding has a lesser effect if either the plume volume or density of ions within the plume is diminished; therefore, if there are fewer ions available to provide shielding, there will be on average a lesser delay between when the ions are desorbed and when their motion is significantly affected by the quadrupole field. It is believed that this is the effect responsible for the trends evident in Figs. 1–3. For series 1, the phase was optimized for maximum signal intensity when the laser fired at −30°, whereas for series 7–11 an insignificant number of ions were trapped when the laser fired at this phase. The ions were then not shielded for as long when the ion production was lowest. Consequently, when produced at −30°, the majority of the ions began to be influenced by the quadrupole field at a phase angle less than 90° and were not trapped, as predicted by the simulations.

Corroboration of the mechanism proposed above can be had if it can be successfully applied to interpret the results from other LD-ITMS studies, such as several of the observations described in our recent article [2] that have yet to be fully explained. Referring to Fig. 3 in the other work, it can be seen that the peak phase angle for $q_z = 0.1$ is approximately −30°, the same value as for series 1 in Fig. 2 here. In fact, the signal versus phase plots are nearly identical for these two trials that were acquired for similar experimental conditions (including the total ion yield—observe the correspondence between the integrated signal intensities for each series). Moreover, as q_z increases, the same trends that accompany decreased ion production in Fig. 2 here are evident in the other Fig. 3: the phase angle of peak trapping efficiency shifts towards larger values, the width of the distributions of acceptable phases narrow, and there is a constant cutoff phase value around 90°. It is known, though, that the trends in the other Fig. 3 are not artifacts of decreased ion production at higher q_z values.* Therefore, the trends must be due to the effects of the increasing rf amplitude, which mimic the effects that accompany a reduction in the quantity of ions desorbed.

The close similarity of the two experiments is readily interpretable: the trends in both cases are believed to stem from a reduction in the effects of Debye shielding. The delay between when the laser fires and when the ions experience the quadrupole

* The data were acquired in order of high to low q_z values to ensure that any decrease in ion production after many laser shots did not overemphasize the increase in signal intensity observed at low q_z.

field is reduced not only if fewer ions are produced, but also if the ions are dispersed at a faster rate. As stated previously, the rate of deshielding is directly related to the magnitude of the electric field, which is in turn proportional to q_z. Thus, we can expect that the distribution of delays will be shifted towards lower values as the rf amplitude increases, which is exactly the effect observed.

3.2. Dependence of the phase for optimum trapping efficiency on the location of the laser focal area on the sample probe

When performing any of the various methods of laser desorption mass spectrometry, it is frequently desirable to translate either the focusing lens, or the sample itself, so that the laser light impinges on different areas of the sample surface. This is because many samples are quickly depleted after only a few laser shots, or else they may have uneven surface distributions. In order to attain sufficient ion production from the samples, both of these eventualities may then require that new portions of the sample surface be exposed to the laser at regular intervals. Compared to most other sample types, the polythiophene films used here as laser desorption standards provide ion production that is superior in terms of both longevity and consistency; however, even polythiophene samples are imperfect. This means that occasionally the probe must be turned to expose a new surface to the laser, or alternatively the focusing lens can be translated slightly so that the laser focal spot impinges on a new position on the probe. Significantly, for laser desorption from a probe inserted through the ring electrode of a quadrupole ion trap, it has heretofore been assumed that this type of adjustment does not affect the relationship between trapping efficiency and the phase angle at which the laser fires.

To investigate the possibility that the inconsistencies described earlier stemmed in part from deviation in the location of the laser focal point, series of signal versus phase data were acquired with the lens set to two different lateral positions. Initially, the lens position was set so that the laser impinged on the outer edge of the probe tip. Since the diameter of the tip is

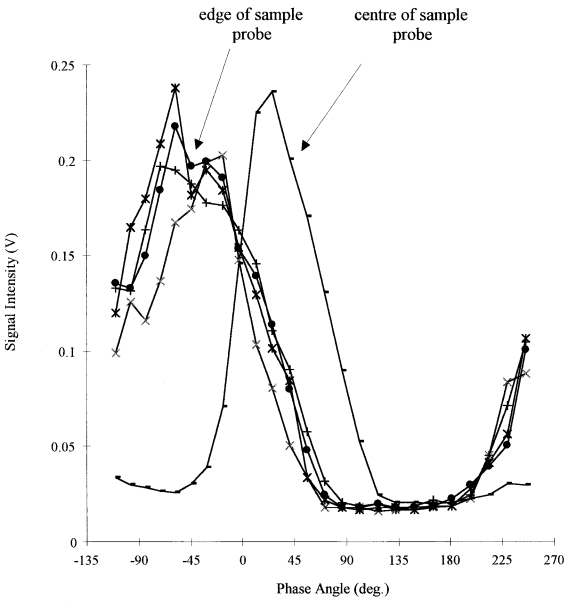

Fig. 4. Integrated signal for the TBA molecular ion acquired as a function of phase angle. Series of data were collected with the laser focal area situated at two different positions on the probe tip. The first position was located at the edge of the probe tip. The second position was translated over 0.5 mm, so that ion production came from near the probe tip center.

1.8 mm, and the width of the focal spot at the sample surface is 0.4 mm, it is believed that for the first lens position the desorbed ions originated from an area that was offset 0.5–0.9 mm towards one endcap in the axial dimension. The intensity of the focused beam is not homogeneous over its 0.4 mm length, though, so ion production may have been concentrated from localized spots within the broader focal area. The initial radial (r) and axial (z) coordinates of the ions when they are desorbed at this position are thus $r = r_0 = 10$ mm and somewhere between $z = 0.5$ and 0.9 mm. Fig. 4 displays a summary of the signal versus phase data that were acquired with the lens at this position. After collecting several series of data, the lens was translated to a new position 0.5 mm toward the trap center axis. All the data summarized in Fig. 2 came from this spot on the sample ($r = 10$ mm and $z = 0.0$–0.4 mm). In order to compare the results from each position, a data series collected at the second position has been included in Fig. 4. The

signal intensities from the various series have not been normalized; rather, those series selected for comparison between the positions were chosen on the basis of their similar intensities, so that differences in ion production between series could be eliminated as a variable.

Examining the results displayed in Fig. 4, there is a striking phase shift evident in the data for the two lens positions. All the series acquired for the first lens position have similar values for the phase for best trapping (~−45°), as well as for the cutoff phase where ions are no longer trapped (~70°). The series displayed for the second position has an optimum phase value of ~25° and a cutoff phase of ~115°, results that are entirely consistent with those summarized in Fig. 2. The discrepancy between the cutoff phases is especially important, because it suggests that, in the absence of ion–ion interactions, the optimum phases for trapping will still be substantially different. This indicates that the relationship between trapping efficiency and phase depends strongly on the position of the probe from which the ions originate.

To date, there is insufficient information available to elucidate the mechanism responsible for this dependence. Ion injection simulations have been run where the ions were injected from positions that were displaced from the axial origin of the trap, but in no case was a shift in the peak phase for trapping observed. The only difference noted in the simulations was an increase in the axial displacement of the ions over the course of their trajectories.* Some other factor is then probably responsible for the variation observed in Fig. 4. One possibility is that the effect is due to irregularities in the quadrupole field caused by the spatial configuration of the probe tip: the probe tip is flat across its surface, and there is a separation between the edge of the tip and the ring electrode (the gap is 0.35 mm all the way around the probe tip). At the edge of the probe tip the strength of the electric field may be very high, so ions created there may experience different conditions than those formed near the center of the probe. In any event, it is impossible to state with certainty what the cause of this effect is; the results indicate, however, that the area from where the ions are created from the probe is another important parameter for laser desorption in the quadrupole ion trap.

3.3. Study of the effects of the helium bath gas pressure on LD-ITMS

Thus far in the discussion, the effects of the helium buffer gas on the trapping mechanism have been ignored. It has long been recognized that to trap ions injected with some energy from the trap periphery, some means of damping the motion of the ions must be employed (although some researchers employing special trapping methods appear to have obviated this requirement [21]). Typically, a bath gas of helium at approximately 1 mTorr is utilized to effect this damping. For the simple trapping method under consideration here, no signal is observed for laser desorbed ions if a bath gas is not present. In the search to discover the factors responsible for the fluctuation in the phase dependence of trapping efficiency, an experiment was performed to see if variations in the pressure of helium were somehow responsible for the discrepancies noted.

Fig. 5 displays three series of signal versus phase data acquired for three different pressure conditions. The first series was collected when the pressure of helium was extremely high, approximately 8 mTorr. This was the highest pressure that could be maintained in the vacuum chamber before the turbopump switched off (which did in fact occur immediately after this series was collected). The spectral series acquired at high pressure is characterized by prominent TBA molecular ion peaks, with relatively small signals from the fragment ions. At lower pressures, Fig. 5(b) and (c), fragmentation of the desorbed ions becomes increasingly prominent, as the molecular ion signal is greatly reduced and the intensity of the peaks due to lower mass fragments increase. This type of behavior has been observed in the past by McLuckey

* In the absence of scattering effects, ions injected from the ring have large trajectories in only the radial dimension-ions injected with zero initial displacement or velocity in the axial dimension experience no acceleration toward the endcaps, and thus the axial component of their trajectories is zero.

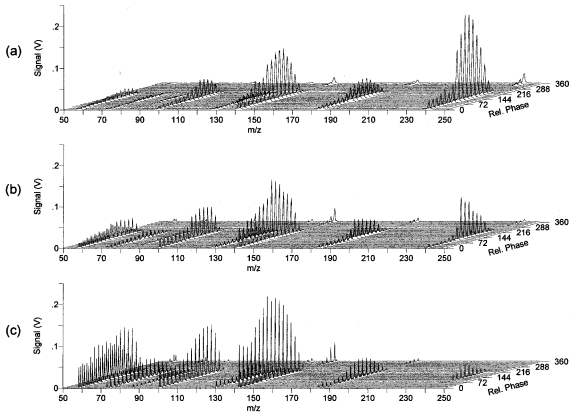

Fig. 5. Series of laser desorption mass spectra of TBA acquired as a function of the phase angle at the time of the laser pulse. The pressure of helium within the manifold was varied between the series shown. The data in plots (a)–(c) were collected for helium pressures of 8, 2, and 0.5 mTorr, respectively. The calibration of the *z* axis is relative.

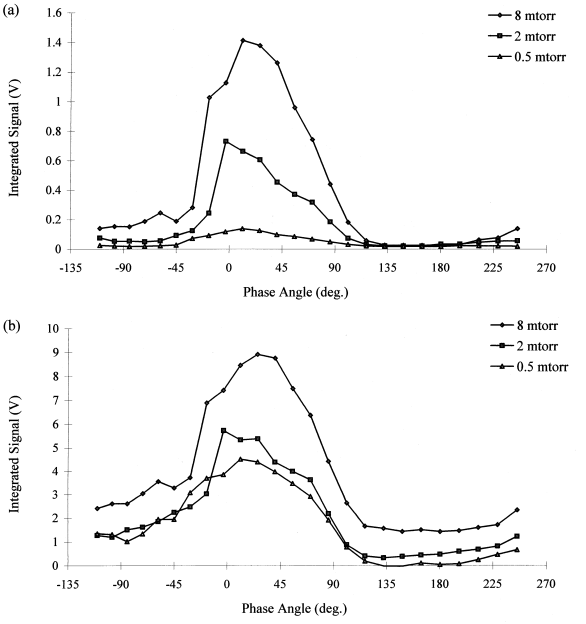

Fig. 6. (a) Integrated signal for the TBA molecular ion plotted as a function of phase from the three series displayed in Fig. 5. (b) Total ion current plotted as a function of phase for the same three data series. The decrease in signal intensity for the TBA molecular ion as pressure lowers is partially compensated by the increase in the fragment ion signals.

et al. [22], who presumed that higher pressures limit the kinetic energies that the ions acquire from the rf field, thereby reducing the energy of collisions between the injected ions and the background gas. Apparently, at high pressures, the reduction in collision energy more than compensates for the increased collision frequency, because the diminishment of fragmentation is indicative of a decrease in the average internal energy deposited into the ions as they are injected, or desorbed in this case.

Fig. 6 displays the integrated intensity for the *m/z* 242 molecular ion signal, as well as the integrated signal for the entire mass spectra (total ion current), plotted as a function of phase for the three different pressures. The total ion currents do not increase nearly as much with pressure as do the TBA molecular ion signals. As shown in Fig. 5, the reduction of the TBA molecular ion signal at lower pressures is at least partially matched by the substantial increase in the signal intensities of the fragment ions. This suggests that much of the apparent increase in trapping efficiency commonly associated with high pressure ion trap operation may in fact be due to reduction of fragmentation upon injection/desorption, rather than simply more effective containment. Close inspection of Fig. 5(a) and (b) reveals that the resolution of the peaks is severely degraded at the higher pressures. Clearly, though, the presence of helium does improve LD-ITMS performance, because as the pressure is lowered beyond 0.5 mTorr, the molecular ion signal disappears altogether for TBA, followed soon after by the signal from the fragment ions.

Returning to the original problem of the variation in the phase relationship, the data summarized in Fig. 6 indicate that there is no significant deviation in the dependency of TBA signal on phase, so the pressure of the background gas is not a factor in this regard.

4. Conclusion

The data presented within this article illustrate how the phase dependence of LD-ITMS signal intensity is a function of the number of ions produced during the

laser pulse, as well as on the position of the probe from which the ions originate. The mechanisms proposed to explain the experimentally observed trends rely upon conjecture regarding phenomena accompanying ion production from laser desorption. Before the trapping process for laser desorbed ions can be described with complete certainty, it will be necessary to successfully elucidate specific details of the laser desorption process that remain unknown. Nevertheless, the effects observed are real enough, and the mechanisms proposed to explain them, although speculative, are plausible and consistent with the information available to date.

The effects discussed portend real problems that will complicate practical applications of LD-ITMS, especially those requiring quantitative information. First and foremost, the strong dependency of the optimum phase value for trapping on total ion yield and on the location of the laser focal area make it impossible to predict what the best phase will be for a given experiment. Moreover, even if a pre-experiment is performed to learn the optimum phase, there is no guarantee that the value selected will remain the optimum value. When a continuous series of data is collected, the ion signal will eventually disappear, and there may be no sure method to determine the extent to which this is due to loss of ion production or to the advent of an unfavorable shift in the optimum phase for trapping. Adjusting the phase at which the laser fires may temporarily increase the signal intensity, but this will also eliminate any possibility of employing calibration curves for quantitative analysis. Summing up, in order to optimize the signal for LD-ITMS, it is presently necessary to empirically discover the best phase angle for trapping not only at the beginning of each experiment, but also at periodic intervals throughout the experiment.

Regarding the best pressure of helium to use for LD-ITMS, evidently a relatively high pressure (>1 mTorr) is best to minimize fragmentation and to optimize trapping efficiency, but these benefits come at the expense of overloading the vacuum system, increased risks of arcing, and severe losses of resolution. Accordingly, it is not possible to state an optimum value for routine use, because a trade-off will need to be made depending on the relative importance of these factors.

References

[1] D. Robb, M.W. Blades, J. Am. Soc. Mass Spectrom. 8 (1997) 1203–1205.
[2] D.B. Robb, M.W. Blades, Rapid Commun. Mass Spectrom., in press.
[3] V.M. Doroshenko, T.J. Cornish, R.J. Cotter, Rapid Commun. Mass Spectrom. 6 (1992) 753–757.
[4] G.C. Eiden, A.W. Garrett, M.E. Cisper, N.S. Nogar, P.H. Hemberger, Int. J. Mass Spectrom. Ion Processes 136 (1994) 119–141.
[5] R.R. Vargas, R.A. Yost, in Practical Aspects of Ion Trap Mass Spectrometry: Ion Trap Instrumentation, R.E. March, J.F.J. Todd, (Eds.), CRC, Boca Raton 1995, Vol. 2, pp. 217–234.
[6] M. Blades, D. Robb, FACSS XXIV, Providence, RI, 1997, Paper 531.
[7] D. Robb, M.W. Blades, Proceedings of the 45th ASMS Conference on Mass Spectrometry, Palm Springs, CA, 1997, paper MPD 077.
[8] D.B. Robb, Ph.D. Dissertation, University of British Columbia, Vancouver, 1998.
[9] C. Weil, M. Nappi, C.D. Cleven, H. Wollnik, R.G. Cooks, Rapid Commun. Mass Spectrom. 10 (1996) 742–750.
[10] L. He, D.M. Lubman, Rapid Commun. Mass Spectrom. 11 (1997) 1467–1477.
[11] F.F. Chen, Introduction to Plasma Physics and Controlled Fusion, 2nd ed., Plenum, New York, 1983.
[12] S.C. Beu, C.L. Hendrickson, V.H. Vartanian, D.A. Laude Jr., Int. J. Mass Spectrom. Ion Processes 113 (1992) 59–79.
[13] D.A. McCrery, E.B. Ledford Jr., M.L. Gross, Anal. Chem. 54 (1982) 1435–1437.
[14] G.C. Stafford Jr., P.E. Kelley, J.E.P. Syka, W.E. Reynolds, J.F.J. Todd, Int. J. Mass Spectrom. Ion Processes 60 (1984) 85–98.
[15] G. Tourillon, in Handbook of Conducting Polymers, T.A. Skotheim, (Ed.), Marcel Dekker, New York, 1986, Vol. 1, pp. 293–350.
[16] R.J. Cotter, A.L. Yergey, Anal. Chem. 53 (1981) 1306–1307.
[17] L.V. Vaeck, J.D. Waele, R. Gijbels, Mikrochim. Acta III (1984) 237–257.
[18] M. Yang, J.P. Reilly, J. Phys. Chem. 94 (1990) 6299–6305.
[19] R.C. Beavis, B.T. Chait, Chem. Phys. Lett. 181 (1991) 479–484.
[20] G.R. Kinsel, D.H. Russell, J. Am. Soc. Mass Spectrom. 6 (1995) 619–626.
[21] V.M. Doroshenko, R.J. Cotter, Rapid Commun. Mass Spectrom. 7 (1993) 822–827.
[22] S.A. McLuckey, G.L. Glish, K.G. Asano, Anal. Chim. Acta 225 (1989) 25–35.